Anomalous electron transport in doped uncompensated p-GaAs/AlGaAs quantum wells: evidence of virtual Anderson transition

2008 J. Phys.: Condens. Matter 20 395216

(http://iopscience.iop.org/0953-8984/20/39/395216)

IOP PUBLISHING JOURNAL OF PHYSICS: CONDENSED MATTER

J. Phys.: Condens. Matter **20** (2008) 395216 (9pp) doi:10.1088/0953-8984/20/39/395216

Anomalous electron transport in doped uncompensated p-GaAs/AlGaAs quantum wells: evidence of virtual Anderson transition

N V Agrinskaya[1], Y M Galperin[1,2], V I Kozub[1] and D V Shamshur[1]

[1] A F Ioffe Physico-Technical Institute, St-Petersburg 194021, Russia
[2] Department of Physics and Center for Advanced Materials and Nanotechnology, University of Oslo, PO Box 1048 Blindern, 0316 Oslo, Norway

Received 17 April 2008, in final form 7 August 2008
Published 1 September 2008
Online at stacks.iop.org/JPhysCM/20/395216

Abstract

For highly doped uncompensated p-type layers located within the central part of GaAs/AlGaAs quantum wells, we observed the activated low-temperature behavior of conductivity. The low values of the activation energy, $\varepsilon_4 = (1–3)$ meV, cannot apparently be ascribed to standard mechanisms. We attribute this behavior to the existence of a narrow band of extended states near the maximum of the density of states in the impurity band. The Hubbard repulsion prevents metallic transport of holes over these states. However, the minority carriers—electrons—supplied by background defects and situated at low temperatures within the tail of the impurity band can be activated to the above mentioned band of extended states. We refer to this behavior as the *virtual Anderson transition* since the conductance is maintained by the extended states formed within the impurity band though the conductivity is not metallic. The low-temperature ($T \lesssim 4$ K) conductance is strongly non-Ohmic: the I–V curves are S-shaped that leads to a breakdown behavior. We explain the observed low threshold fields ($\lesssim$10 V cm^{-1}) by the fact that we are dealing with the impact ionization of the electrons from the states below the chemical potential to the band of extended impurity states situated close to the chemical potential, the ionization energy being small.

1. Introduction

Although the problem of metal-to-insulator transition (MIT) has been discussed for many years, it is still far from being completely understood. In particular, we can mention recent debates concerning MIT in 2D systems apparently observed in some systems with high mobility (for a review see for example [1]). The situation seems not to be fully understood yet and the nature of the 'metal' state is still questionable. At the same time, several indications of a crossover between the insulator-like and metal-like behavior were observed in different doped quantum-well structures [2–5].

In our view, a productive approach to the problem is to start from systems with hydrogen-like localized states originating from intentionally introduced dopants. This situation can be the case in a quantum well with a selectively doped central part. If the structure is not intentionally compensated, then the disorder is weak and is mostly controlled by the background defects with a concentration independent of doping. Thus the relative degree of disorder for the samples close to MIT is expected to be less for p-doped materials, where the critical concentration of dopants is larger and the relative number of the background defects compared to dopants is less.

This paper summarizes our results on the metal–insulator crossover in 2D p-doped uncompensated GaAs–AlGaAs quantum-well structures. In such structures, the background compensating defects (with a concentration by 2–3 orders of magnitude less than the concentration of dopants) are most probably situated far from the 2D layer of dopants [6]. As a result, firstly, the impurity band is narrow since the concentration of charged defects is small; secondly, the chemical potential is located not far from the center of the impurity band [6] in contrast to 3D structures where it is

located very deep in the band tail. As we will show, the Anderson transition in such structures takes place at a lower concentration than the Mott transition.

Recently we reported observation of activated low-temperature conductivity in Be-doped uncompensated GaAs/AlGaAs single and multiple quantum wells with anomalously small activation energies (more than an order of magnitude smaller than the Bohr energy of the dopant) [7]. This behavior cannot be associated with the nearest neighbor hopping because it was accompanied by an *increase* in the Hall mobility with a decrease of temperature contrary to the theoretical prediction [8] for the nearest neighbor hopping. Thus we believe that in that work, as well as here, we face a *novel* phenomenon—activation of minority carriers to a band of extended states (BES) existing near the center of a narrow impurity band. Such a band can exist in a narrow window of concentrations, which are less than those described by the Mott criterion of MIT for the case of a wide impurity band due to smaller scatter of the site energies. However, the upper and lower Hubbard bands in this case are still not overlapping and all the sites within BES are singly occupied by the holes. The conductivity over these states is possible only due to activation of electrons (resulting from weak background compensation) from the states below the chemical potential. The more detailed considerations are given in section 3. We call this mechanism the *virtual Anderson transition* [7] exploiting the analogy to the virtual thermodynamic phase transition with negative transition temperature considered as a precursor of a true phase transition where accomplished new phase is not observed.

In the present paper, in addition to the data concerning the temperature dependence of conductivity and mobility, we also present new data on the sign and magnitude of the low-temperature Hall effect, as well as the data on non-Ohmic low-temperature transport characterized by a S-shaped I–V curve. The Hall coefficient at low and high temperatures has different signs indicating different signs of dominating carriers at low and high temperatures. Note that these phenomena are observed in a relatively narrow region of the dopant concentration where the band of extended states is already created but the two Hubbard bands still do not overlap. We will show that all these results are consistent with our model of the virtual Anderson transition in the narrow impurity band. The paper is organized as follows. In section 2 we report the experimental results, which are then discussed in section 3. The main results are summarized in section 4. The criterion for impact ionization leading to pronounced nonlinear behavior is considered in the appendix.

2. Experiment

We study multilayered structures grown by MBE as described in [9]. The structures contained 1 or 5 GaAs quantum wells with widths 15 nm separated by 100 nm barriers of $Al_{0.3}Ga_{0.7}As$. The middle region of the wells (5 nm) was doped by p-type impurities (Be); the volume impurity concentration was controlled during the growth and varied from 1×10^{18} atoms cm^{-3} up to 2×10^{18} atoms cm^{-3}.

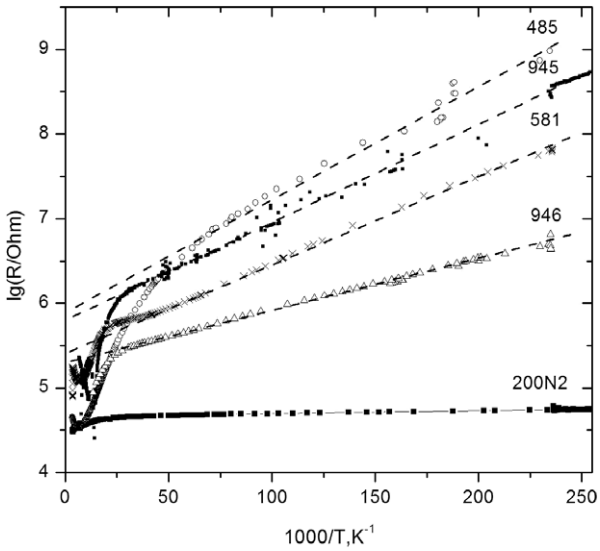

Figure 1. Temperature dependences of the resistivity. The sample numbers according to table 1 are shown near the curves. For comparison we also show a similar curve for the sample 200N2 of [3], which is in the regime of weak localization.

Table 1. Parameters of the samples. Here ε_1 is the high-temperature activation energy, ε_4 is the low-temperature activation energy, σ_0 is the pre-exponential factor of ε_4 conductivity.

No	No of wells	Well width (nm)	$p_{300\,\mathrm{K}} \times 10^{-12}$ (cm^{-2})	ε_1 (meV)	ε_4 (meV)	σ_0 (e^2/h)
581	1	15	1	15	2	0.1
945	1	15	1.5	14	2.5	0.03
946	1	15	1.7	13	1.5	0.1
485	5	15	1.5	13	2.5	0.03

The critical concentration corresponding to the Mott criterion of the metal–insulator transition in the bulk p-type GaAs is 2×10^{18} cm^{-3}. So the bulk concentration of acceptors in our samples is of the order of or a bit less than the critical one. The compensation is supposedly controlled by the background defects situated both at the edges of the quantum wells and within the barriers, the compensation degree being small, $K = N_D/N_A < 0.01$. The parameters of the samples are given in table 1.

Shown in figure 1 is the temperature dependence of the resistance. Since we studied square samples these data provide the sheet resistivity. At low temperatures (10–1.3 K) it obeys the Arrhenius law, $R \propto \exp(\varepsilon_4/T)$, with an anomalously low activation energy, $\varepsilon_4 \approx$ 1–3 meV. The activation energy, ε_4, decreased with an increase of the acceptor concentration (see curves for the samples 945 and 946). As can be estimated from the curves in figure 2, the pre-exponential factor in conductance, σ_0, is only 10–30 times less than the quantum limit, $e^2/h = 4 \times 10^{-5}\ \Omega^{-1}$.

Figure 1 demonstrates the temperature dependences of the Hall mobility, μ, for these samples. Note that in the temperature domain 10–40 K the mobility *decreases* with temperature. This behavior is contrary to the theoretical prediction [8] of an exponential *increase* for the nearest

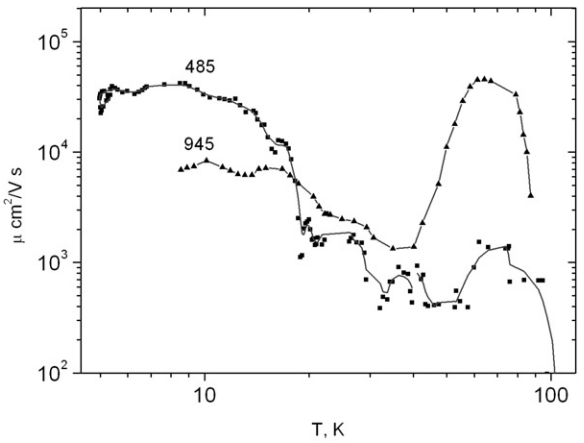

Figure 2. Temperature dependences of the Hall mobility for two samples showing the ε_4-conduction.

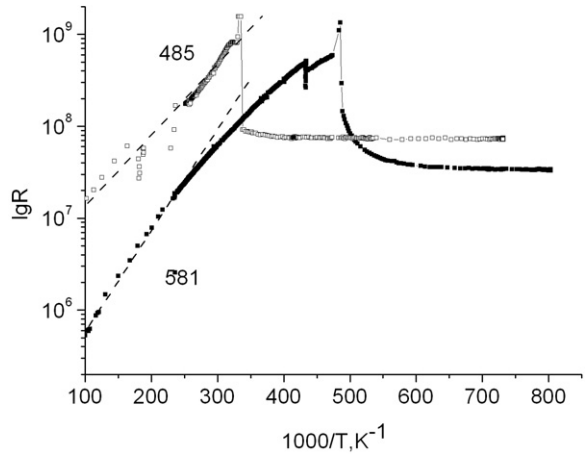

Figure 3. Temperature dependences of resistance of the samples 485 and 581 measured at constant current $I = 0.1$ nA.

neighbor hopping. We believe that the experimentally observed behavior can be explained by scattering of delocalized electrons by acoustic phonons [10, 11].

At higher temperatures, 40 K $< T <$ 100 K, the Hall mobility increases with temperature while for $T >$ 100 K it again starts to decrease. While the behavior at $T >$ 100 K is clearly explained as a result of scattering of the holes within the valence band by optical phonons, the increase of Hall mobility at intermediate temperatures needs a special analysis which will be given later.

Temperature dependences of the Hall coefficient for these samples at high temperatures ($T =$ 300–50 K) are described by the Arrhenius law, corresponding activation energies, $\varepsilon_1 \sim \varepsilon_0/2$, being given in table 1. Here ε_0 is the acceptor Bohr energy. This is related to the fact that at temperatures >50 K the concentration of holes in the valence band turn out to be larger than the concentration of compensating defects, and the chemical potential shifts to the position $\varepsilon_0/2$. The low-temperature behavior of the Hall coefficient will be discussed in detail later.

Let us now turn to the nonlinear effects in conductivity. figure 3 shows temperature dependences of resistance for the samples 485 and 581 measured in a regime of constant current. As temperature decreases, both the samples exhibit sharp transitions from insulating behavior (Arrhenius law), to the metallic behavior, the resistance decreasing by 1.5–2 orders of magnitude. We attribute these transitions to an electrical breakdown occurring when the voltage drop across the sample (increasing with the temperature decrease under condition of constant current) exceeds some critical value. The transition temperatures differed for different samples, 3 and 2.4 K, respectively. This temperature is supposedly controlled by the temperature-dependent voltage drop across the sample.

Figure 4 shows I–V curves of the samples (obtained in the regime of constant I) at $T =$ 4.2 K. The curve clearly demonstrates an S-shaped region. One notes that the breakdown takes place at relatively weak electric field (<10 V cm^{-1}).

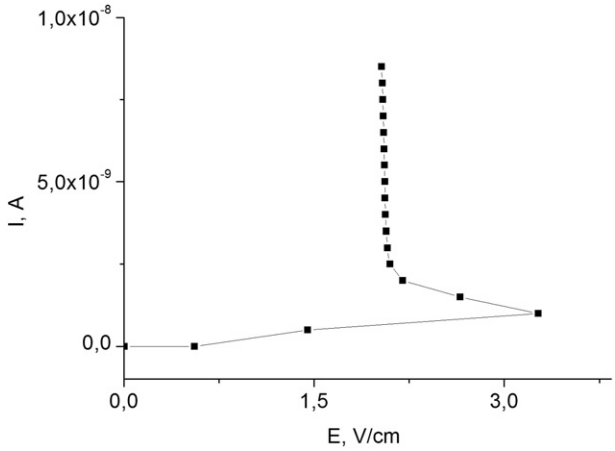

Figure 4. I–V curve for sample 485 at 4.2 K.

3. Interpretation and discussion

As well known, the Anderson transition is a single-particle problem depending on the interplay between the overlap between the localized states and the spread of their energies. The Mott transition, in contrast, is sensitive to the occupation numbers and is inherently dependent on the on-site (Hubbard) repulsion. The Anderson scenario of MIT is considered to be the case in standard 3D doped samples with an intermediate degree of compensation. In this case there exists a clear mobility edge separating strongly and weakly localized states. The MIT takes place when the Fermi level crosses the mobility edge. In contrast, in weakly compensated materials with a conventional impurity band the MIT combines features of both scenarios and is sometimes called the Mott–Anderson transition. Indeed, for the wide impurity band with a width of the order of the Bohr energy of an isolated impurity the criteria of the Mott and Anderson transitions actually coincide. Namely, at the same concentrations the overlap integrals become comparable both to the spread of the on-site energies determined by the inter-site Coulomb interaction, and the on-site (Hubbard) repulsion.

However, these equalities are modified in the case of the narrow impurity bands characteristic for weakly compensated systems with a weak disorder. In this case the spread of the on-site energies can be much less than the Hubbard energy. Consequently, these states can cease to meet the criterion of the Anderson localization. As a result, the *extended states* can exist though the double occupation is still not allowed. One can expect that the MIT in such systems should significantly differ from that in the conventional impurity band. The presence of the narrow band of extended states (BES) would not manifest itself at all in the absence of compensation since this band is fully occupied by the majority carriers (in our case, holes). The transport of the majority carriers is blocked at temperatures less than the Hubbard energy, $T \lesssim U$, since the width of the BES is considered to be less than U. Consequently, the system remains insulating despite the presence of the BES.

Background donors produce electrons, which can occupy the acceptor states. One can consider these electrons as the 'minority carriers' inside the (acceptor) impurity band. Assuming that the net distance between the background donors from the 2D layer is d one obtains that the Fermi level is located at distance of

$$\varepsilon_F \approx e^2/\kappa d \tag{1}$$

below the center of impurity band [6]. One can expect that at small dopant concentrations when all the states are localized, and the conductance due to this 'minority carriers' is the standard nearest neighbor hopping with the activation energy $\varepsilon_3 = \varepsilon_F \approx e^2/\kappa d$. For our samples this estimate gives $\varepsilon_3 \approx$ (2–6) meV.

Increase of the dopant concentration leads to a subsequent increase of the overlap integral. As a result, a narrow BES can be formed. The criterion for such Anderson-like delocalization in a narrow band can be written as [7]

$$N_A a^2 \geqslant \alpha/\ln[\varepsilon_0/(\delta\varepsilon)] \tag{2}$$

where N_A is the dopant (acceptor) concentration, a is the localization length and α is a numerical factor. For the 2D case, $\alpha = 0.15$. It is assumed that the width ($\delta\varepsilon$) of the impurity band is much less than the Bohr energy ε_0. In this case the conductivity is dominated by an activation of the electrons, i.e., *minority* carriers from the background dopants to the corresponding mobility edge. The corresponding scheme is presented in figure 5. Note that the activation energy, ε_4, turns out to be much less than the Bohr energy ε_0.

One could expect that increase of the compensation degree (for the given N_A), leading to an increase of the electron concentration, would shift the chemical potential to the center of the acceptor band. Correspondingly, at some concentration the chemical potential would cross the mobility edge resulting in metallic conductivity. However the position of the chemical potential is still controlled by equation (1) provided the concentration of compensating defects $N_c \ll N_A$. At the same time, when N_c becomes comparable to N_A strong disorder resulting from the charged defects of both kinds inevitably increases $\delta\varepsilon$ up to values comparable to ε_0 when the criterion (2) can break.

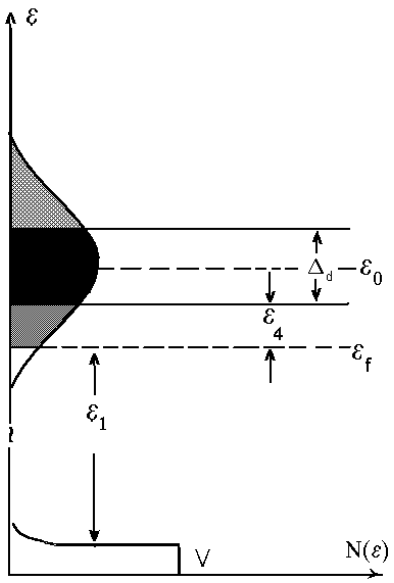

Figure 5. Schematic diagram of the density of states in the samples with narrow impurity band. The dark area represents the band of extended states (BES) with the width Δ_d; ε_F is the Fermi energy measured from the center of the impurity band, ε_0 is the distance between the center of the impurity band and the valence band, while ε_1 and ε_4 are the activation energies.

As a result, the presence of the BES in a narrow impurity band can be seen only through transport of the activated minority carriers. The discussed activated transport can be considered as a precursor of true metallic conductance, which would appear with an increase of N_c in the absence of the enhancement of $\delta\varepsilon$. This enhancement 'kills' the expected Anderson transition in conductance, which would take place provided the states at the Fermi level are extended.

As was noted earlier, the observed decrease of the Hall mobility with temperature is incompatible with the nearest neighbor hopping and leads us to the conclusion that the activated minority carriers are delocalized. Indeed, then the observed behavior can be explained by scattering of delocalized carriers by acoustic phonons. This assumption does not contradict the observed increase of the Hall mobility with temperature at high temperatures. We attribute this increase to the contribution of carriers activated to the valence band, where scattering on charged impurities prevails. As known, scattering on acoustic phonons is very sensitive to the effective mass of the carriers. In particular, as it was noted above, the ratio of the relaxation times with respect to ionized impurities scattering and acoustic phonon scattering is proportional to m^2.

Previously we estimated the effective mass in the impurity band for the sample with a metallic conductivity over the upper Hubbard band [5]. The estimate was based on comparison of conductivities along the valence and the impurity band. The estimate explicitly exploited the Fermi statistics of the carriers within the impurity band. We concluded that the corresponding effective mass exceeded the valence-band mass by factor of 3. Unfortunately, here we cannot apply the same procedure since the electrons within the BES obey Boltzmann statistics.

However, we expect that the excess factor in our case must be larger than estimated in [5] since typically the effective mass increases with a decrease of the band width. Note that an electron mass within the impurity band substantially exceeding (by factor of 5) the mass in the conducting band has been reported [14]. The dominant role of phonon scattering in low-temperature mobility was also reported for high-mobility 2D structures, see, e.g., [10, 11]. The high mobility ($\geqslant 10^4$ cm^2 V^{-1} s^{-1}) observed in our samples can be explained by the fact that the disorder potential is weak since the samples are uncompensated and the localized states are mostly neutral.

Additional support for the above picture is given by the opposite signs of the Hall coefficient at 4.2 and 300 K. Indeed, the BES is equivalent to the existence of two mobility edges separating the extended states from the localized tail states. Near the lower edge, the states are *electron-like*, i.e., they have positive effective mass (see figure 5). The states around the upper mobility edge are *hole-like*, see, e.g., discussion in [15]. At low temperatures the carriers in the BES are mostly located close to the lower mobility edge, and the Hall effect is electron-like. At high temperatures the main contributors to the Hall effect are holes in the valence band. At intermediate temperatures, 40 K $< T <$ 100 K, both holes in the valence band and electrons within the BES contribute to the Hall coefficient. In this case, the Hall coefficient and mobility can be written as

$$R_{\mathrm{H}} = -\frac{1}{ec}\frac{n\mu_n^2 - p\mu_p^2}{(n\mu_n + p\mu_p)^2}, \qquad \mu = R_{\mathrm{H}}(n\mu_n + p\mu_p) \quad (3)$$

where n and p are electron and hole concentrations while μ_n and μ_p are their partial mobilities. Obviously, both n and p increase with temperature. The behavior of μ_n and μ_p in the intermediate region is not as clear due to the possible contribution of the scattering by charged centers resulting from activation of the holes to the valence band. However, as follows from the experimental results, at some temperature R_{H} vanishes. According to equation (3), the Hall mobility should also vanish. We believe that it explains the observed minimum in the temperature dependence of μ at $T \sim 50$ K.

As for the breakdown behavior, it can hardly take place in the regime of hopping conductivity. Indeed, the hopping conductivity in finite electric fields was studied earlier for a similar group of samples [9]. According to that work, the hopping conductivity strongly increases with the electric field. However, this increase was gradual, in agreement with theoretical prediction [12], and no breakdown-like behavior was observed.

One can attribute the observed breakdown to impact ionization of the acceptors to the valence band. However, in this case the increase in conductivity is expected to be much more pronounced than the one observed experimentally. In addition, for our case of relatively deep localized states, the breakdown field is expected to be at least an order of magnitude larger (see, e.g., [13]) compared to the experimentally observed.

We assume that as a result of the breakdown states most of the initially localized minority carriers are ionized to the extended states. Thus we have a unique possibility to find their sign and total concentration (equal to the concentration of the background compensating defect) by studies of the Hall coefficient for this excited metallic state. The results for the sample 485 at 4.2 K (which according to figure 4 corresponds to the breakdown state) are presented (figure 6) compared to the data obtained at 300 K. As it is clearly seen, the sign of the Hall coefficient at 300 K is *opposite* to its sign at low temperatures in figure 6. At the same time, the concentration estimated from the Hall coefficient at low temperatures appears to be 2–3 orders of magnitude lower than that at $T = 300$ K. From this fact one can conclude that the total concentration of the electrons is also 2–3 orders of magnitude lower than the dopant concentrations, the compensation degree being 10^{-2}–10^{-3}. This estimate is compatible with the carrier concentration obtained from the Hall conductance in the low-Ohmic state (figure 6).

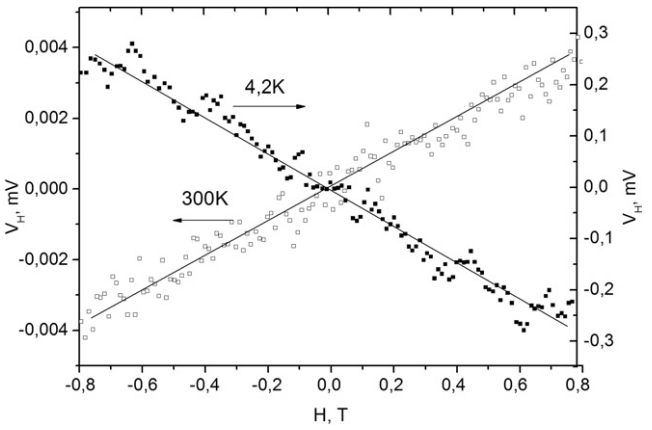

Figure 6. Hall voltage as a function of magnetic field for $T = 4.2$ and 300 K for a fixed direction of the current $I = 2$ nA.

We believe that the observed non-Ohmic behavior is also compatible with the presence of the BES. Indeed, the impact ionization to the valence band should be excluded by the fact that the conductance in the low-Ohmic state is still much less than the high-temperature conductance dominated by the valence band. Then, the electric fields in our experiments are orders of magnitude less than necessary for impact ionization of deep centers [13]. In addition, extremely small heat release (note that the breakdown behavior occurs at currents less than 1 nA!) excludes heating.

Consequently, we conclude that the observed non-Ohmic behavior results from the impact ionization of the electrons localized in the tail of the impurity band to the BES. The important factor is the presence of energy gap between the Fermi level and the mobility edge separating the strongly localized states and the BES in the impurity band. The concentration of the localized states in this gap, see figure 5, is much larger than the electron concentration in the BES. Consequently, these states trap electrons belonging to the BES with a much larger probability than the background dopants, which have produced these electrons. We believe that it is the impact ionization of these centers by delocalized electrons that is responsible for the breakdown with very low threshold field. Indeed, these states are much closer to the mobility

edge than the deep tail states. A similar mechanism involving the 'intermediate' states located between an ionized level and bottom of the conduction band and leading to formation of S-shaped I–V curves has been considered before [16].

More detailed estimates allowing for both the kinetics of impact ionization and a nonequilibrium electron distribution in strong electric fields are presented in the appendix. The critical field, E_1, for the ionization from the Fermi level to the BES is estimated as

$$eE_1(l_i l_{e-ph})^{1/2} \sim \varepsilon_4. \quad (4)$$

Here l_i is the (transport) electron mean free path while l_{e-ph} is the partial mean free path due to electron–phonon scattering. Both quantities should be calculated for the electron energy close to ε_4. This equation has a clear physical meaning. Indeed, $l_d \equiv (l_i l_{e-ph})^{1/2}$ is just the distance covered by a diffusive electron during the inelastic mean free time. Thus the breakdown occurs in the electrical field, E_1, able to supply an electron by the extra energy, $eE_1 l_d$, close to the activation energy, ε_4, from the Fermi energy to the BES. The critical field, E_2, describing ionization from the 'intermediate' states, is given by a similar estimate. However, the energy ε_4 in this case should be replaced by a smaller energy distance, ε_g (see the appendix). Consequently, $E_1 > E_2$.

Now let us provide estimates for the relevant parameters. The experimental low-temperature mobility increases with a temperature decrease and almost saturates at $T \equiv T_s \lesssim$ 10–15 K at a value of $\sim 10^4$ cm^2 V^{-1} s^{-1}. Assuming $m \sim 10^{-27}$ g (that is few times larger than the valence-band effective mass) and using the experimental value of the saturated mobility, one estimates the transport time as $\tau_i \sim 10^{-11}$ s. To estimate the electron–phonon relaxation time at the crossover temperature we assume that the contributions of the electron–phonon and impurity scattering are equal. Such an estimate leads to a relaxation time of 4×10^{-11} s. Since we are interested in the relaxation time at the mobility edge, $\varepsilon = \varepsilon_m \sim 1$ meV, we rescale the relaxation time to this energy using the scaling, $\tau_{e-ph}^{-1} \propto \varepsilon^2$, see [17]. Estimating the electron velocity for the energy $\sim\varepsilon_m$ as 3×10^6 cm s^{-1} we get $E_1 \approx 10$ V cm^{-1}. The electric field E_2 is expected to be several times smaller, firstly, due to the fact that $\varepsilon_g < \varepsilon_m$, and secondly, due to electron–electron interaction (see the appendix). The above order-of-magnitude estimates agree with experimental results presented in figure 6.

Additional indirect support of the conclusion that we do not deal with impact ionization of holes to the *valence band* follows from figure 3. One can see that the conductance of the low-Ohmic state is of the order of the Ohmic conductance at $T \sim 10$ K, and is somewhat smaller than the conductance at intermediate temperatures 20–40 K where the dominating process is electron activation to the BES. In the case of activation to the valence band, one could expect the resulting conductance to be of the same order of magnitude as the high-temperature conductance, i.e., several orders of magnitude larger. Comparing the values of conductance at 10 K and in the interval 20–40 K one concludes that only a fraction of localized electrons are ionized to the BES.

Note that both the observed and the estimated threshold field are surprisingly low. We know few references reporting S-shaped I–V curves at such a low fields, except for the case of shallow donors [18]. This fact allows us to rule out the Mott-type scenario of MIT. Indeed, the observed activation energy in the high-temperature domain almost coincides with the ionization energy of an isolated (rather deep) acceptor. However, for the Mott transition one would expect the Fermi level to be situated somewhere between the energies of single occupied and doubly occupied states. We can also conclude that the observed ε_4-conductivity cannot be attributed to the nearest neighbor hopping (ε_3-channel).

Thus, the combination of observed behaviors strongly supports the scenario discussed above, which we call the virtual Anderson transition. Let us stress once more specific features of this phenomenon. The conventional Anderson transition is a typically single-particle phenomenon. In our case, the transport of the majority carriers (holes) is blocked by Coulomb effects even though the single-particle wave functions are extended. The charge transfer via the band of extended states becomes possible *only* due to activation of minority carriers (electrons) from the localized states belonging to the tail of the impurity band. Another difference between the above scenario and the conventional Anderson transition is that in the latter case the transition takes place when the Fermi level crosses the mobility edge. In our case, the Fermi level does not cross the mobility edge. As a result, the transport remains activated, the activation energy being small. As shown in [7], the critical concentration of acceptors allowing the above scenario is given by equation (2) and turns out to be less than that for the conventional Mott transition by a factor $\ln[\varepsilon_0/(\delta\varepsilon)]$. Due to this factor the virtual Anderson transition can take place in our samples, which have too low an acceptor concentration to exhibit the conventional Mott–Anderson transition.

In connection with observed behaviors, one can also discuss the Lifshits scenario of localization [19]. The criterion for this mechanism to be dominant differs from the Mott criterion by numerical factors, which are beyond proper control. In addition, this criterion is sensitive to the assumption of a uniform spatial distribution of dopants, which is not the case for our samples. Since it is known that deviations from purely random impurity distribution suppress the Lifshits transition we believe that it is irrelevant for our samples.

4. Conclusions

To conclude, the observed dependences of the conductance and Hall effect on temperature and applied voltage confirm the existence of a band of extended states in the narrow impurity band. Since the Fermi level is located below this band, the low-temperature transport is due to activation of minority carriers to this band. Both the activation energy and threshold voltage for non-Ohmic behavior turn out to be anomalously small. This scenario, which we call the *virtual Anderson transition*, seems to be typical for moderately doped intentionally non-compensated materials. At large dopant concentrations obeying the standard Mott criterion one expects the conventional Mott–Anderson transition. However at intermediate concentration one expects suppression of the

virtual Anderson transition due to an increase of disorder (in particular, due to partial overlapping of the lower and upper Hubbard bands and formation of charged doubly occupied and empty states). Thus the crossover between the two regimes can be a complex one.

We would like to note that, although it seems as if we deal with rather old subject, we are not aware of any papers reporting similar phenomena. Here we mean the combination of (i) Arrhenius behavior of conductivity with anomalously small activation energies in a wide temperature domain; (ii) gradual change of the Hall coefficient from positive to negative values with a decrease of temperature; (iii) breakdown behavior with S-shaped I–V curves at anomalously small voltages and currents, which does not lead to restoration of the conductivity to its high-temperature value. To the best of our knowledge, our theoretical concept of the virtual Anderson transition (a formation of extended states within the narrow impurity band which still does not lead to metallic behavior of conductivity) has not been discussed earlier.

Acknowledgments

We are grateful to A E Zhukov for manufacturing the structures and to A S Ioselevich for discussion. This work was supported by the Russian Foundation for Basic Research (project No. 06-02-17068) and by the Norwegian Research Council.

Appendix. Criterion for impact ionization

We consider impact ionization of localized minority carriers—electrons—situated deeply in the tail of the impurity band (with a concentration N_1, controlled by compensating defects) by extended minority carriers to delocalized states with energies higher than the mobility edge ε_m. We also take into account the localized states (with concentration $N_2 \gg N_1$) having energies between ε_m and ε_F. These states are occupied by holes, so they can serve as traps for electrons.

Let us use a simple 3-level model including the band of extended states, localized 'tail' states and 'intermediate' states having the same energy, $\varepsilon_g < \varepsilon_m$. In what follows we will show that this model provides an adequate qualitative description of the realistic situation.

Denoting the concentrations of the extended and trapped electrons as n and $\tilde{n}$, respectively, we have the following rate equations:

$$\dot{n} = -B_R n(N_2 + n) + A_I n\mathcal{F}_2\tilde{n} + A_I n\mathcal{F}_1(N_1 - \tilde{n} - n),$$
$$\dot{\tilde{n}} = -\tilde{B}_R\tilde{n}(n + \tilde{n}) - A_I\mathcal{F}_2 n\tilde{n} + B_R n(N_2 - \tilde{n}). \tag{A.1}$$

Here B_R describes recombination of the electrons to any localized states, $\tilde{B}_R$ describes the recombination of electrons from the intermediate states to their initial positions, A_I is a coefficient of impact ionization, $\mathcal{F}_1$ and $\mathcal{F}_2$ are the relative numbers of mobile electrons with kinetic energies larger than ε_m and ε_g, respectively:

$$\mathcal{F}_1 = \frac{1}{n}\int_{\varepsilon_m}^{\infty} d\varepsilon\, \nu(\varepsilon) f(\varepsilon), \qquad \mathcal{F}_2 = \frac{1}{\tilde{n}}\int_{\varepsilon_g}^{\infty} d\varepsilon\, \nu(\varepsilon) f(\varepsilon). \tag{A.2}$$

Here $\nu(\varepsilon)$ is the density of states, while $f(\varepsilon)$ is the electron distribution function. In general, the coefficients A_I, B_R are energy dependent. However we will neglect these dependences since the width of the impurity band is not much larger than ε_m, and thus the relative variation of ε at energies higher than the threshold value ε_m is not large.

From the first of equations (A.1) one concludes that since $N_2 \gg N_1$ the solution with $n = \tilde{n} = 0$ is stable with respect to small fluctuations provided $E < E_1$ where E_1 satisfies the equation

$$A_I\mathcal{F}_1 N_1 = B_R N_2. \tag{A.3}$$

Another stationary solution with finite n and $\tilde{n} = 0$ is

$$\tilde{n} \simeq B_R N_2/A_I\mathcal{F}_2, \qquad n = N_1 - \tilde{n}. \tag{A.4}$$

Here we use the relations $A_I\mathcal{F}_2 \gg B_R$ (which holds at electric fields of the order of E_1), $\tilde{B}_R \ll B_R$, and $N_2 \gg N_1$. This solution is stable until $\tilde{n} \leqslant N_1$, or

$$A_I\mathcal{F}_2 N_1 \geqslant B_R N_2, \tag{A.5}$$

which defines another critical field, E_2. Since $\varepsilon_m > \varepsilon_g$ it is expected that for a given field $\mathcal{F}_2 \gg \mathcal{F}_1$. Thus the value of E_2 can be smaller than E_1 and this is the case for our samples.

Thus we deal with two branches: the one corresponding to $n = \tilde{n} = 0$, which is stable with respect to small fluctuations at $E < E_1$, and the solution given by equation (A.4). For electric fields $E \sim E_1$, the second solution corresponds to almost complete ionization of the electrons to the BES. However this solution can exist at smaller fields, i.e., in the domain $E_2 < E < E_1$, where the two solutions coexist and are stable with respect to small fluctuations.

To complete the analysis one should estimate the parameters B_R and A_I, as well as the relative numbers of the localized and extended electrons, $\mathcal{F}_{1,2}$. The parameter A_I is just the product $v\sigma_I$ where σ_I is the ionization cross-section. The latter (for 2D) can be roughly estimated as $\sigma_C(\sigma_t^2/\lambda^2)$. Here $\sigma_C \sim (e^2/\kappa\varepsilon)^{1/2}$ is the geometrical cross-section of a Coulomb scattering of an electron with kinetic energy $\varepsilon > \varepsilon_m$ by a charged center, κ being the dielectric constant, σ_t is the cross-section of elastic scattering of an electron by the trap, while λ is a typical electron wavelength. It can be roughly estimated as $\lambda^{-2} \sim N_3$ where N_3 is the concentration of the delocalized states. The elastic cross-section σ_t can be estimated from known values of electron mean free path l_i as $\sigma_t \sim (N_2 l_i)^{-1}$. Note that partial cross-section can be smaller than that given by the above estimate if electron momentum relaxation is dominated by other mechanism. As for B_R, we shall consider recombination due to phonon emission. In this case the recombination process involves simultaneous interaction of an electron with a phonon and a (neutral) trap center. One can estimate the recombination cross-section $\sigma_R \sim B_R/v$ as $\sigma_t^2/v\tau_{e-ph,s}$. Correspondingly, the estimates of the critical fields E_1 (E_2) can be rewritten as

$$\frac{B_R N_2}{A_I\mathcal{F}_{1(2)}} N_1 \simeq \frac{N_2}{N_3 N_1 v\tau_{e-ph,s}\sigma_C\mathcal{F}_{1(2)}} = 1. \tag{A.6}$$

Assuming that $N_2 \sim N_3$ one concludes that our scenario can hold provided

$$N_1 v\tau_{e-ph,s}\sigma_C > 1 \tag{A.7}$$

since in any case $\mathcal{F} < 1$. As can be readily estimated, $\sigma_C \sim 2 \times 10^{-5}$ cm while $v\tau_{e-ph,s} \sim 10^{-4}$ cm. Thus this criterion is met for $N_1 > 0.5 \times 10^9$ cm^{-2}.

Now we have to address the relative concentrations, $\mathcal{F}_{1,2}$, as functions of applied electric field. For that we will assume that electron transport can be described by conventional diffusion equations. Strictly speaking, this assumption is not true for energies close to the mobility edge. However, we believe that it will allow us to make correct order-of-magnitude estimates. Neglecting electron–electron interaction (that is appropriate for sufficiently small n) we get the following equation for the electron distribution function:

$$\left[D_E + \frac{T^2}{\tau_{e-ph,T}}\right]\nabla_\varepsilon f + \frac{T_s}{\tau_{e-ph,s}} f = 0. \tag{A.8}$$

Here the first term describes diffusion of an electron along the energy axis due to combined acceleration by the applied electric field ($D_E \sim e^2E^2v^2\tau_i$) and quasi-elastic scattering by acoustic phonons with energy $\sim T$. The last term corresponds to the spontaneous emission of the phonons with the typical energy of the delocalized electrons, which can be roughly estimated as the saturation temperature, T_s.

While estimating the electron–phonon relaxation time for a 2D electron gas one should take into account that the normal component of the phonon momentum is not conserved. As a result, at low temperatures $\tau^{-1}_{e-ph,T} \propto T^3\varepsilon^{-1/2}$, which is similar to the electron–phonon relaxation rate in 3D metals for $\hbar\omega \sim T$. However, for relatively small energies, $\varepsilon < (ms^2W)^{1/2}$ (where s is a sound velocity while W is an energy of lateral quantization, which in our case of 2D impurity band is of the order of the Bohr energy) $\tau^{-1}_{e-ph,s} \propto \varepsilon^2$ [17], while the typical value of ε is T_s.

The solution of equation (A.8) depends on the relation between D_E and the phonon contribution to energy diffusion. If the phonon contribution dominates, then the distribution function is equilibrium, $f \propto e^{-\varepsilon/T}$. In the opposite case when

$$eEl_d \gg T \tag{A.9}$$

the distribution is essentially strongly nonequilibrium,

$$f \propto \exp\left[-\int^{\varepsilon} d\varepsilon' \frac{\varepsilon'}{(eEv)^2\tau_i\tau_{e-ph,s}}\right]. \tag{A.10}$$

Substituting here $\tau_i \propto \varepsilon^{-d}$ with $d = 2$ and assuming $\varepsilon \approx \varepsilon_m$ we get:

$$f(\varepsilon) \propto \exp\left[-\frac{\varepsilon^2}{5(eEv)^2\tau_i(\varepsilon)\tau_{e-ph,s}}\right]. \tag{A.11}$$

This function is nearly constant at $\varepsilon < \varepsilon_*$ defined by the equation where

$$5(eEv)^2\tau_i(\varepsilon_*)\tau_{e-ph,s} = \varepsilon_*^2 \tag{A.12}$$

and very rapidly decays at $\varepsilon > \varepsilon_*$. One can see that the inequality (A.9) is equivalent to the inequality $\varepsilon_* \gg T$. Since an equilibrium phase at $T \to 0$ corresponds to $n = 0$, the threshold field and, correspondingly, $\mathcal{F}_1$, is related to a distribution given by equation (A.11) which can be modeled as $\mathcal{F}_1 = \theta(\varepsilon_* - \varepsilon_m)(\varepsilon_* - \varepsilon_m)/\varepsilon_*$. Thus E_1 can be estimated from an equality $\varepsilon_* \simeq \varepsilon_m$ which gives

$$eE_1(l_{i,m}l_{e-ph,m})^{1/2} \sim \varepsilon_m. \tag{A.13}$$

Indeed, for $E > E_1\mathcal{F}_1 \sim 1$, and the condition (A.6) holds. Note that ε_m by definition coincides with the activation energy ε_4. The estimate of E_2 is a similar one and we have $E_2 < E_1$ because of the replacement of ε_m by $\varepsilon_g < \varepsilon_m$ in equation (A.13).

If n is high enough, the energy relaxation is dominated by electron–electron rather than by electron–phonon processes. In this case,

$$f(\varepsilon) = e^{-\varepsilon/T_e} \tag{A.14}$$

where T_e is the temperature of the electrons. However, the energy transfer from the whole electron system to the bath is still due to electron–phonon processes. The effective electron temperature T_e which is established in the system can be derived from the energy balance between the energy gain from electric field, $\sigma E^2 = n(eE)^2\tau_i/m$ and its decay to the thermal bath $\sim n(T_e - T)/\tau_{e-ph}$. Here σ is the conductivity. Thus we have

$$E^2\gamma(T_e) = \frac{T_e}{T} - 1, \qquad \gamma \equiv \left.\frac{e^2\tau_i\tau_{e-ph}}{mT}\right|_{\varepsilon=T_e}. \tag{A.15}$$

As follows from equations (A.14) and (A.12), the estimate for T_e is the same as for ε_* except for numerical factors, which are beyond the full control. Both quantities characterize a typical electron energy, which is controlled by the energy balance between electrons and is independent of the efficiency of electron–electron processes. However the high-energy asymptotic behavior of the distribution function strongly depends on the electron–electron scattering. Namely, in the absence of this scattering the decay of $f(\varepsilon)$ at $\varepsilon \geqslant \varepsilon_*, T_e$ is much more rapid—since, in contrast to equation (A.10), the electron–electron scattering tends to establish the Boltzmann distribution with effective electron temperature. As a result, the effective impact ionization by the latter distribution can be supported at an electric field somewhat weaker than that following from the distribution given by equation (A.11).

Finally, let us discuss the validity of our model, which ignores the possibility of a continuous spectrum, ε_i, of the intermediate states and ascribing to all of them the same value, $\varepsilon_i = \varepsilon_g$. Following the above assumption of energy-independent B_R and A_I one concludes then the rhs of equation (A.5) is independent of ε_i. At the same time, the function $\mathcal{F}_2$ decreases with energy. For the following discussion, it is convenient to introduce the normalized probability, $\mathcal{P}(\varepsilon_i)$, to have an intermediate state with energy ε_i. In this case the quantity $\mathcal{F}_2(E, \varepsilon_g)$ in the lhs of equation (A.5) should be generalized as $\Phi(E) \equiv \int_i d\varepsilon\, \mathcal{P}(\varepsilon)\mathcal{F}_2(E, \varepsilon)$ where the integration is performed over the band of intermediate states. For a given electric field, $\mathcal{F}_2(E, \varepsilon)$ is a decreasing function of ε and one can expect that for any $\varepsilon < \varepsilon_m$ the inequality $\mathcal{F}_2(E_1, \varepsilon) > \mathcal{F}_1$ is met. Since the probability $\mathcal{P}(\varepsilon)$ is also a decreasing function one concludes that $\Phi(E_1) > \mathcal{F}_1$. On the other hand, the quantity $\Phi(E)$ *increases* with electric

field, so one can expect that it breaks down at some $E_2 < E_1$. This conclusion qualitatively agrees with that made on the basis of the 3-level model.

References

[1] Kravchenko S V and Sarachik M P 2004 *Rep. Prog. Phys.* **67** 1
Shashkin A A 2005 *Usp. Fiz. Nauk* **175** 139
Shashkin A A 2005 *Phys.—Usp.* **48** 129 (Engl. Transl.)

[2] Van Keuls F W, Mathur H and Dahm A J 1997 *Phys. Rev.* B **56** 13263

[3] Hsy S-Y and Valles J M 1995 *Phys. Rev. Lett.* **74** 2331

[4] Havin Yu, Gershenson M and Bogdanov A 1998 *Phys. Rev.* B **58** 8009

[5] Agrinskaya N V, Kozub V I, Poloskin D S, Shamshur D V and Chernyaev A V 2004 *Pis. Zh. Eksp. Teor. Fiz.* **80** 36
Agrinskaya N V, Kozub V I, Poloskin D S, Shamshur D V and Chernyaev A V 2004 *JETP Lett.* **80** 30 (Engl. Transl.)

[6] Ye Q, Shklovskii B I, Zrenner A and Koch F 1990 *Phys. Rev.* B **41** 8477

[7] Agrinskaya N V, Kozub V I and Poloskin D S 2007 *JETP Lett.* **85** 169

[8] Galperin Yu M, German E P and Karpov V G 1991 *Zh. Eksp. Teor. Fiz.* **99** 343
Galperin Yu M, German E P and Karpov V G 1991 *Sov. Phys.—JETP* **72** 193 (Engl. Transl.)

[9] Agrinskaya N V, Kozub V I, Ivanov Yu L, Chernyaev A V and Shamshur D V 2001 *Zh. Eksp. Teor. Fiz.* **120** 480
Agrinskaya N V, Kozub V I, Ivanov Yu L, Chernyaev A V and Shamshur D V 2001 *JETP* **93** 424 (Engl. Transl.)

[10] Stormer H L, Pfeiffer L N, Baldwin K W and West K W 1990 *Phys. Rev.* B **41** 1278

[11] Mendez E E and Wang W I 1985 *Appl. Phys. Lett.* **46** 1159

[12] Shklovskii B I 1979 *Fiz. Tekh. Poluprov.* **13** 93
Shklovskii B I 1979 *Sov. Phys.—Semicond.* **13** 53

[13] Vorob'ev L E, Firsov D A, Shalygin V A, Panevin V Yu, Sofronov A N, Tsoi D V, Egorov A Yu, Gladyshev A G and Bondarenko O V 2006 *Pis. Zh. Tekh. Fiz.* **32** 9–34
Vorob'ev L E, Firsov D A, Shalygin V A, Panevin V Yu, Sofronov A N, Tsoi D V, Egorov A Yu, Gladyshev A G and Bondarenko O V 2006 *Tech. Phys. Lett.* **32** 384 (Engl. Transl.)

[14] Lin I S, Drew H D, Illiades A and Hadjipanteli S 1992 *Phys. Rev.* B **45** 1155

[15] Fritzsche H 1955 *Phys. Rev.* B **99** 406

[16] Scholl E 1982 *Z. Phys.* B **46** 23

[17] Karpus V 1986 *Fiz. Tekh. Poluprov.* **20** 12
Karpus V 1986 *Sov. Phys.—Semicond.* **20** 6 (Engl. Transl.)

[18] Kostial H, Ihn T, Asche M, Hey R, Ploog K and Koch F 1993 *Japan. J. Appl. Phys.* **32** 491

[19] Lifshits I M 1964 *Usp. Fiz. Nauk* **83** 617
Lifshits I M 1965 *Sov. Phys.—Usp.* **7** 571 (Engl. Transl.)